

CHAPTER 4

SYNTHESIS OF CeO₂ NANOPARTICLES BY DIFFERENT EMULSION METHOD

4.1 Introduction

During the past decade, cerium oxide (CeO₂) has been commonly reported to apply as catalyst in a wide variety of reactions involving oxidation or partial oxidation of hydrocarbons. A high oxygen mobility (redox property), high oxygen storage capacity, strong interaction with the supported metal (strong metal–support interaction), and the modifiable ability render this material very interesting for catalysis. Recently, the reactivity toward methane steam reforming with high resistance toward carbon deposition over ceria has been observed. Unfortunately, the steam reforming reactivity over CeO₂ was too low compared to the conventional metallic catalysts. This is mainly due to its low specific surface area, and its high sintering rate at high temperature [47]. In order to minimize the weakness of CeO₂ in terms of its low specific surface area, CeO₂ prepared by microemulsion method in this work should have the high surface area and small particle size.

According to the investigation of He *et al.* [6], it was found that CeO₂ was prepared by coupling route of homogenous precipitation with microemulsion showed high surface area and the nanometer particle size. The study of surfactants type on the average particle size showed that anionic surfactant had the smallest particle size. Hadi and Yaacob [48] studied the preparation of nanocrystalline CeO₂ by mechanochemical and W/O microemulsion. It was found that CeO₂ prepared by microemulsion was more stable than those prepared by mechanochemical method against the effect of heat treatment and the sample has higher specific surface area which was non-porous. In 2008, Sujana *et al.* [49] was prepared nano-ceria by surfactant-mediated precipitation technique in mixed solvent system. The CeO₂ obtained from this method shows good thermal stability and the surface area of sample calcined at 400°C was found to be 133 m²/g.

In this work, the experiment is divided into two parts. Firstly, the three different type of microemulsion (RM, ELM, and CEAs) were used for prepared CeO₂. Then, the suitable method of preparation which provided nanometer particle size, high surface area, and high purity was selected. Secondly, the effect of cerium source, surfactant type, calcination temperature, and the water content on the CeO₂ powder were investigated. X-ray diffraction (XRD), BET surface area analysis and transmission electron microscopy (TEM) were utilized to characterize prepared CeO₂ powder. Thermal analysis was performed by thermo-gravimetric (TGA).

4.2 Objectives

- 1) To synthesize the CeO₂ nanoparticles by different emulsion method.
- 2) To investigate the effect of cerium source, surfactant type, calcination temperature, and the water content on the CeO₂ powder.

4.3 Working scopes

1) Determine the suitable emulsion method (RM, ELM, and CEAs) that gives the smallest particle size and the highest yield, surface area, and purity.

2) At the most suitable preparation method, determine the most suitable conditions of synthesized CeO₂ powder (Cerium sources: (NH₄)₂Ce(NO₃)₆, Ce(NO₃)₃·6H₂O, and CeCl₃·7H₂O, surfactant type: PE4LE, Brij52, Brij96, AOT and CTAB, calcination temperature ranges between 500-900°C, and the water content ranges between 3-7 ml.

4.4 Experimental

4.4.1 Materials

Ammonium cerium nitrate ((NH₄)₂Ce(NO₃)₆) and Polyoxyethylene-4-luaryl ether (PE4LE) were chosen as the cerium source and surfactant for study of the preparation by different three emulsion methods (reversed micelle (RM), emulsion liquid membrane (ELM), and colloidal emulsion aphrons (CEAs)). Hexane (C₆H₁₄) was used as organic solvent and hydrazinium hydrate (N₂H₄·H₂O) was used as reducing agent. The precipitate was washed with ethanol (C₂H₅OH). In CEAs method used Polyoxyethylene sorbitan monooleate (Tween80) to form colloidal gas aphrons. For study the effect of the type of cerium source was used cerium nitrate hexahydrate

($\text{Ce}(\text{NO}_3)_3 \cdot 6\text{H}_2\text{O}$) and cerium chloride heptahydrate ($\text{CeCl}_3 \cdot 7\text{H}_2\text{O}$). The effect of surfactant type was used polyoxyethylene-10-oleyl ether (Brij96V), polyoxyethylene-2-cetyl ether (Brij52), sodium bis (2-ethyl hexyl) sulfosuccinate (AOT), and cetyltrimethylammonium bromide (CTAB). The chemical structures of all surfactants were shown in Figure 4.1.

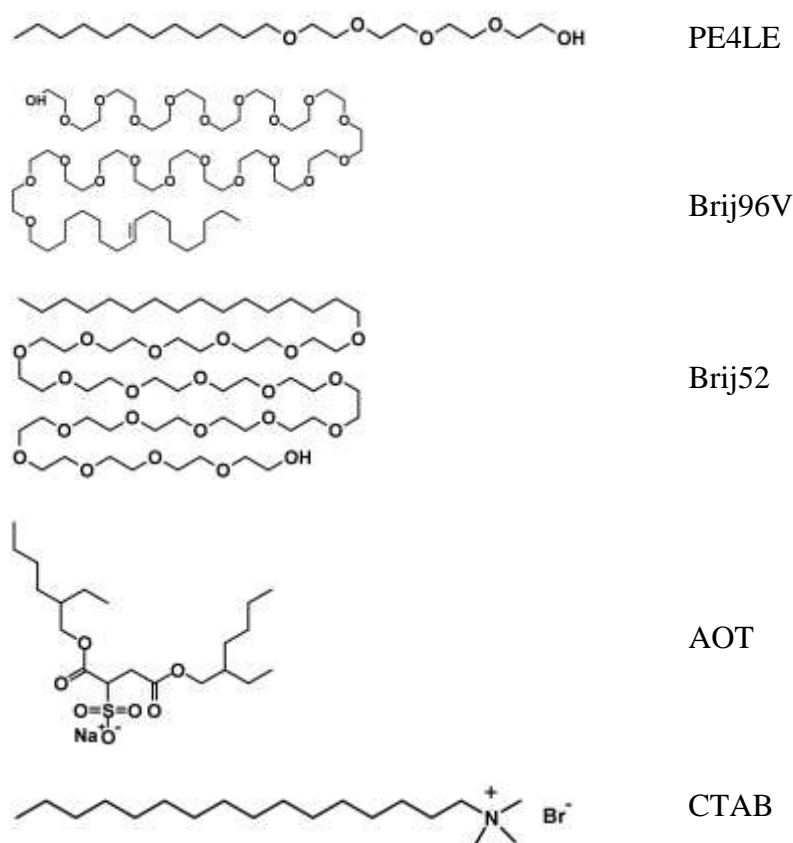


Figure 4.1 The chemical structure of all surfactants.

4.4.2 Preparation of CeO_2 nanoparticles by emulsion method

4.4.2.1 Reversed Micelle (RM)

In typical preparation of CeO_2 nanoparticle, $(\text{NH}_4)_2\text{Ce}(\text{NO}_3)_6$ (2.5 g) was dissolved in 0.1 ml of distilled water and then added into 70 ml of n-hexane. An appropriate amount of PE4LE was added to the solution under vigorous stirred until all $(\text{NH}_4)_2\text{Ce}(\text{NO}_3)_6$ completely dissolved in the solution and transparent microemulsion was obtained. Then $\text{N}_2\text{H}_4 \cdot \text{H}_2\text{O}$ was added into the solution to neutralize the cerium ion in the reverse micelles. The hydrazine in the amount of 5% of total volume is sufficient to ensure that reduction takes place without destroying the isotropic solution. The mixtures of the

solution were centrifuged at 12,000 rpm for 15 min to separate the precipitate from solution. The brown precipitate were washed with ethanol and centrifuged for 2 times in order to completely remove both residual phase and organic phase. The precipitate was dried at 100°C for 1 h and finally was calcined at 500°C for 1 h, then CeO₂ powder was obtained. The schematic procedure is illustrated in Figure 4.2.

4.4.2.2 Emulsion Liquid Membrane (ELM)

An internal phase of W/O emulsion was N₂H₄·H₂O solubilized in the organic membrane phase comprise n-hexane (70 ml) and PE4LE (12 ml). The mixed solution was stirred at 500 rpm for 30 min then the W/O emulsion was obtained. The W/O emulsion was added to an external water phase containing (NH₄)₂Ce(NO₃)₆ (2.5 g) and deionized water. Stirring at vigorously speed was required to disperse W/O emulsion droplet to form W/O/W emulsion. After stirring for 1 h, the mixed solution was turned into dark brown then were placed into centrifuge tube and centrifugation at a speed of 12,000 rpm for 15 min to separated the precipitate from solution. The precipitate were washed with ethanol followed by centrifugation in order to completely remove both residual external phase and organic membrane phase for 2 times. The precipitate was dried at 100°C for 1 h and finally was calcined at 500°C for 1 h, CeO₂ powder was obtained. The schematic procedure is illustrated in Figure 4.3.

4.4.2.3 Colloidal Emulsion Aphrons (CEAs)

An internal phase of W/O emulsion was N₂H₄·H₂O solubilized in the organic membrane phase comprise n-hexane (70 ml) and PE4LE (12 ml). The mixed solution was stirred at 500 rpm for 30 min then the W/O emulsion was obtained. The W/O emulsion was added to the colloidal gas aphrons (CGAs) under stirring at vigorously. The colloidal gas aphrons was prepared by added Tween80 (3 ml) into deionized water (30 ml) and were mixing with a homogenizer at the rotation of 14,000 rpm for 2 min. After stirring for 1 h the colloidal emulsion aphrons (CEAs) was obtained then added an external water phase containing (NH₄)₂Ce(NO₃)₆ (2.5 g) and deionized water into CEAs, the mixed solution was stirred at 500 rpm for 30 min. After stirring the mixed solution was turned into dark brown then were placed into centrifuge tube and centrifugation at a speed of 12,000 rpm for 15 min to separated the precipitate from the solution. The precipitate were washed with ethanol followed by centrifugation for 2 times in order to completely remove both residual external phase and organic membrane phase. The

precipitate was dried at 100°C for 1 h and finally was calcined at 500°C for 1 h, then CeO₂ powder was obtained. The schematic procedure is illustrated in Figure 4.4.

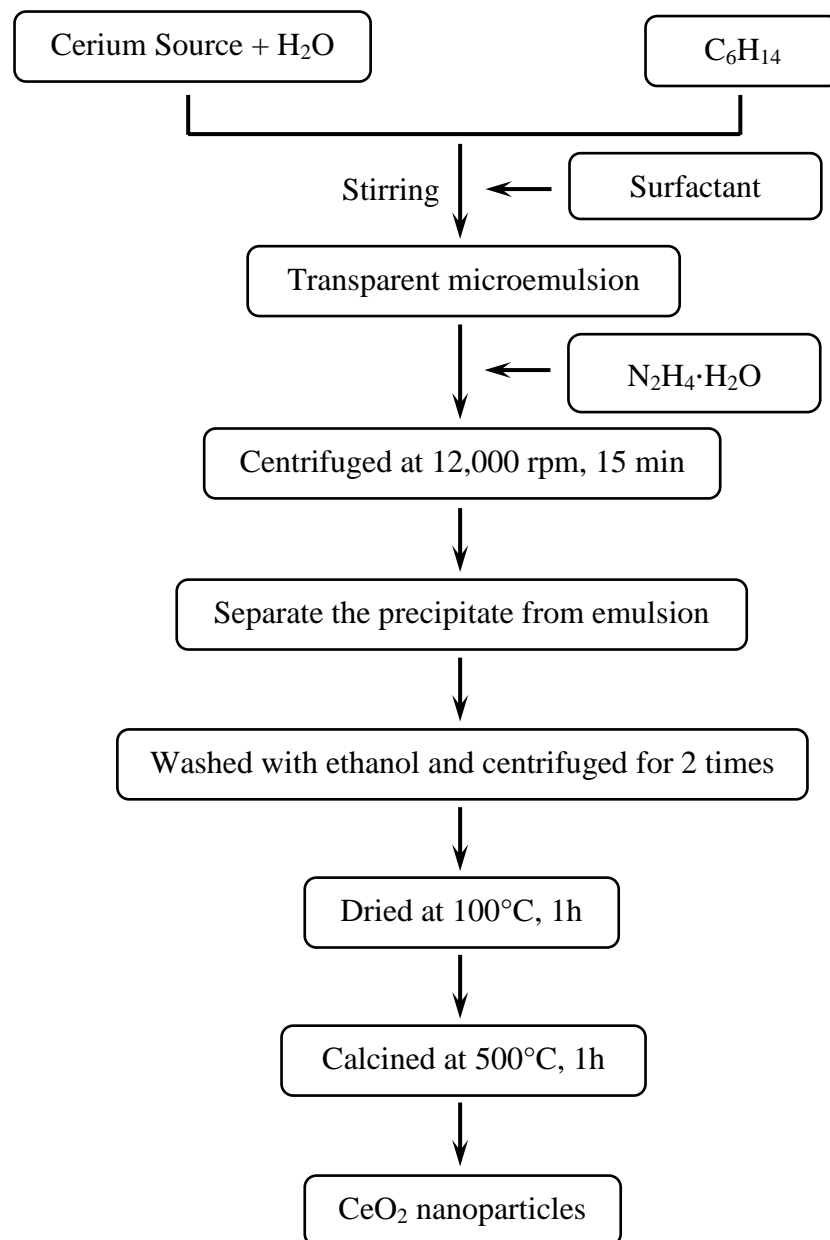


Figure 4.2 The schematic procedure of reversed micelle method.

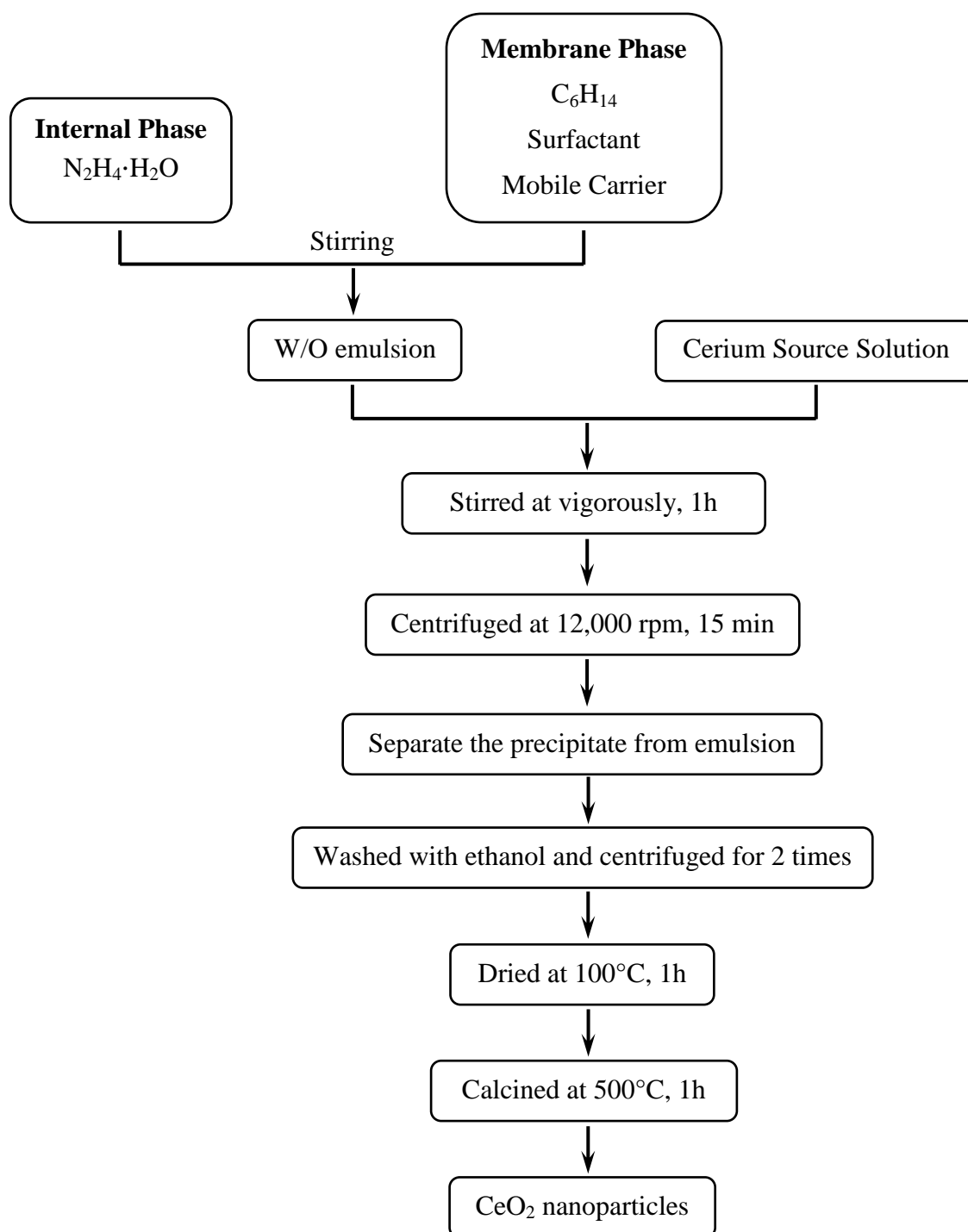


Figure 4.3 The schematic procedure of emulsion liquid membrane.

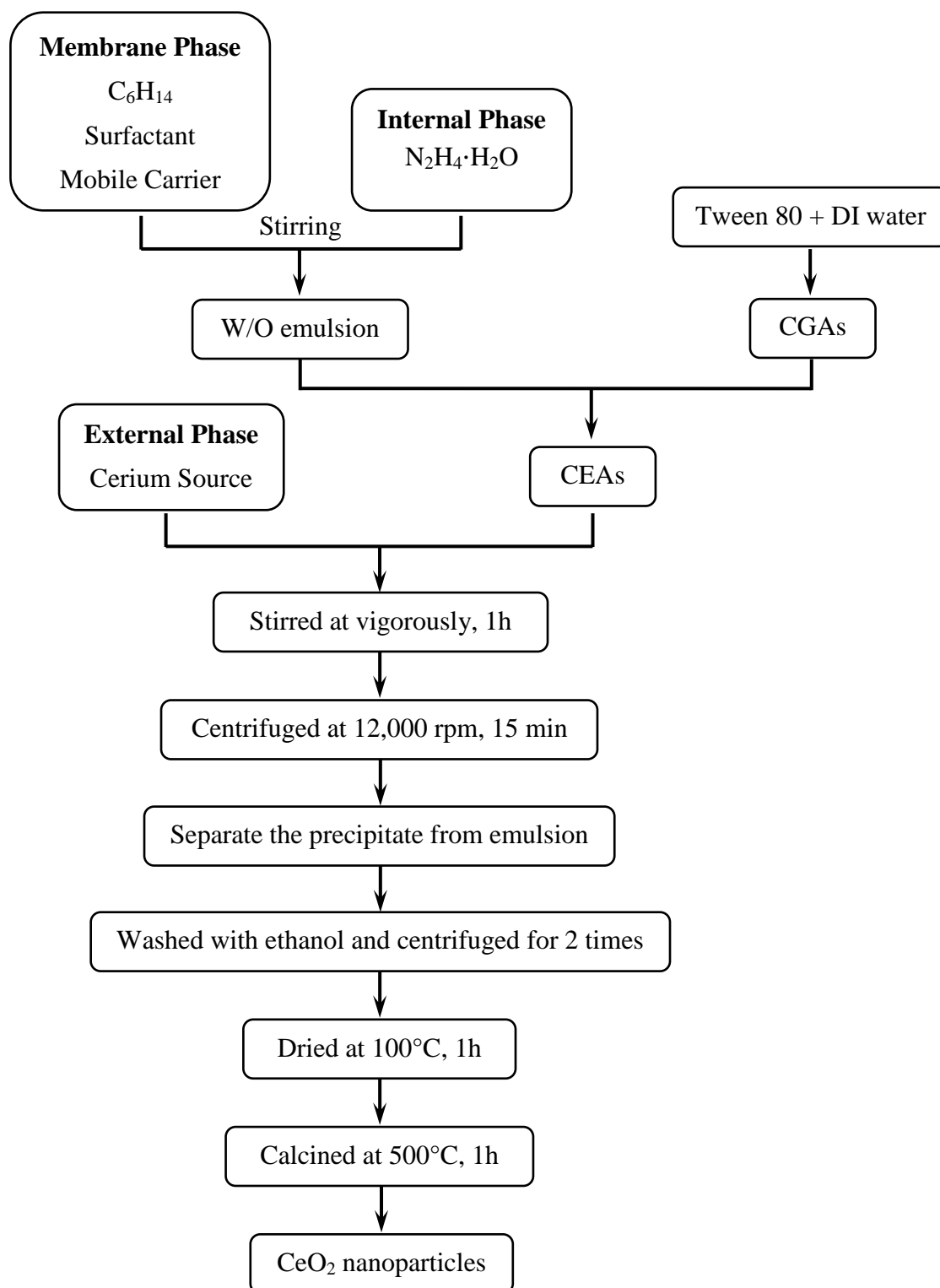


Figure 4.4 The schematic procedure of colloidal emulsion aphrons.

4.4.3 Characterization techniques

The objective of characterization is to examine the powder surface and bulk properties that may provide substantial information about the powder attributes. The information from various characterization tools will significantly improve the understanding of how the physicochemical attributes and powder performances are related. This section give a brief review of the basic concepts of various powder characterization techniques applied in this study, namely XRD, TEM, TGA, nitrogen adsorption/desorption analysis, dynamic light scattering technique, surface area and pore size analysis. Each characterized method is discussed below.

4.4.3.1 X-ray Diffraction

X-ray diffraction (XRD) spectroscopy has been commonly used for crystalline phases identification and the average crystallite size determination in a powder sample. The XRD pattern of material is like a fingerprint of the material. The powder diffraction method is ideally suitable for characterization and identification of a polycrystalline phase. When X-rays interact with a crystalline material, a diffraction pattern is achieved. Every crystalline material gives a pattern; the same material always gives the same pattern. Our aim is to see diffraction pattern is a pure CeO₂ for each preparation method and how the diffraction changed with the factors that studied.

The powder is irradiated with an X-ray of known wavelength, and hence diffraction of the X-ray takes place. The angle at which constructive interference occurs is then measured and the interplanar spacing (d spacing) of the crystals can be evaluated using Bragg's Law [50], as shown in equation (4.1):

$$n\lambda = 2d\sin\theta \quad (4.1)$$

where n is the order of diffraction (integer), λ is the incident X-ray wavelength (Å), d is the spacing between atomic layers in crystal (Å), and θ is the angle between the incidence ray and the scattering plane (degree)

The XRD patterns of the CeO₂ were carried out in a Bruker D8 Discover diffractometer using CuK α radiation ($\lambda = 1.542 \text{ \AA}$) operating at 40 kV and 40 mA, scanned rate at 0.02 degree/step over the angular ranges of $2\theta = 20\text{-}100^\circ$. The crystallite size of sample

powder (d_{XRD}) was estimated by applying full-width-half-maximum (FWHM) of characteristic peak (111) to the Scherrer equation (equation (4.2)) [2]:

$$d_{XRD} = k\lambda/\beta\cos\theta \quad (4.2)$$

Where λ is the wavelength of the X-ray used (Å), β is the half height width of the characteristic peak, θ is the diffraction angle for the (111) plane and k is Scherrer's constant ranging from 0.7 to 1.71. The value of k is used as 0.9 in this study.

4.4.3.2 Thermogravimetric Analysis

The thermal analysis was carried out in order to evaluate the chemical composition of the CeO₂ and elucidate the transformation of crystalline CeO₂. The thermal analysis was performed by thermogravimetrically carried out on a Shimadzu TA-50 thermal analyzer at the heating rate of 10°C/min from room temperature to 1000°C in air atmosphere. Our aim of the TGA analysis is to confirm the purity of synthesized powder of CeO₂.

4.4.3.3 Transmission Electron Microscope

Transmission electron microscope (TEM) is an imaging technique whereby a beam of electrons is transmitted through a specimen, then an image is formed, magnified and directed to appear either on a fluorescent screen or layer of photographic film or to be detected by a sensor such as a CCD camera. TEM investigations were performed on Jeol Model JEM-2100 with 100 kV of accelerating voltage. The samples were prepared by allowing an ethanol suspension of the finely ground powder to evaporate on a copper grid coated with a holey carbon film. The average particle size of synthesized powder from TEM images were measured by IQ Materials Program.

4.4.3.4 Specific surface area, pore volume and nitrogen adsorption/desorption analysis

Since most powder are porous in nature with deep and complex network of pores, the determination of specific surface area is generally considered an important powder characterization. Beside the liquid-solid interface adsorption and the mercury porosimetry, the gas adsorption methods are the most widely used to determine the surface area and pore size distribution. Analysis involves adsorption of nitrogen gas onto the surface and into the pores of outgassed sample. A know amount of nitrogen gas

is added into an evacuated tube containing the sample. The quantity of adsorbed gas and the pressure in the sample tube is incrementally increased with a constant tube temperature. After each dose of nitrogen gas, when the pressure in the sample is equilibrated, the data is recorded. Pressure readings are used to calculate the gas volume adsorbed. The volume of gas adsorbed is measured as a function of relative pressure. Relative pressure is defined as the ratio of pressure in the sample tube to the saturation vapor pressure of adsorbed gas. The sample tube is immersed in a Dewar (vacuum flask) filled with liquid nitrogen to maintain a temperature where liquefaction of nitrogen gas can take place on the sample. The resulting data set is called an adsorption isotherm which is used to calculate the surface area.

The nitrogen adsorption/desorption isotherm was obtained at liquid nitrogen temperature 77 K by using Quantachrome Autosorb-1 surface area and pore size analyzer. Prior to measurement, all synthesized powder were outgas at 250°C under nitrogen flow for 5 h. The total surface area was determined using multi-point BET method by an Autosorb-1 from Quantachrome Instruments, together with the determination of the pore volume as well as the pore size distribution of the sample. Our aim of the nitrogen adsorption/desorption analysis is to assess how the specific surface area, pore volume, and pore size of the synthesized powders varied with the preparing conditions.

4.4.3.5 Dynamic light scattering technique

Dynamic light scattering technique (DLS) has been commonly used for measured the size and zeta-potential to optimize stability and shelf life and speed up formulation development. The emulsion systems were characterized by dynamic light scattering using a Zetasizer nano ZS from Malvern Instrument. Our aim of dynamic light scattering is to measured the size of emulsion droplet prepared by different methods.

4.5 Results and discussion

4.5.1 Methods of Preparation

Figure 4.5 shows the XRD patterns of the products obtained from different method of preparation. All the reflection in Figure 4.5 can be indexed to pure crystalline CeO₂. The characteristic peaks corresponding to (111), (200), (220) and (300) planes are

located at $2\theta = 28.78^\circ$, 33.13° , 48.12° and 56.81° , respectively and no impurity peaks are observed in the patterns. The peaks are close to the ones of the face centered cubic fluorite structure of CeO_2 with lattice parameter is 5.4113\AA (standard data JCPDS 34-0394). However, the peaks in Figure 4.5 (c) obtained from CEAs are broadened more than from ELM and RM, which is in a good agreement with the crystallite sizes of CeO_2 obtained from CEAs are smallest.

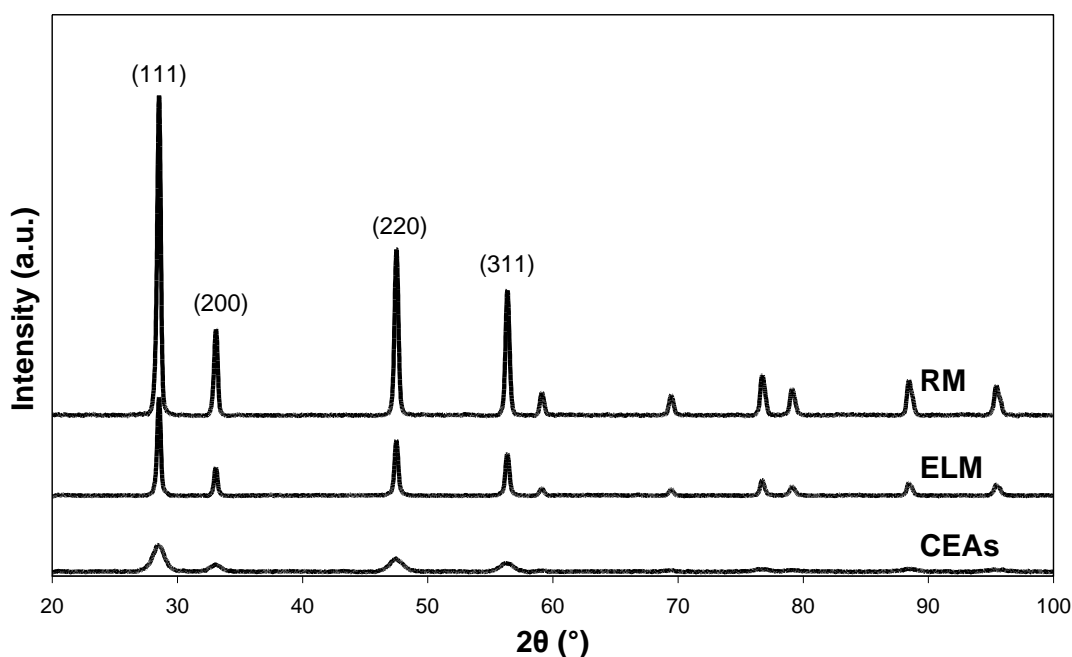


Figure 4.5 XRD patterns of CeO_2 prepared by (a) RM, (b) ELM, and (c) CEAs.

Figure 4.6 shows the TEM micrographs of CeO_2 obtained from preparation by different method. It is evident from the figure that the particles were small in size and uniform in shape. The average particle size of CeO_2 obtained from RM, ELM and CEAs are 9.4, 5.8 and 4.7, respectively. However, this result shows that the average particles size of CeO_2 obtained from CEAs (in Figure 4.6 (c)) are the smallest.

Considering the average particle size of CeO_2 obtained from different method but the same starting material, it was found that the average particles size of CeO_2 obtained from CEAs are smallest. The particles size of prepared by emulsion method were generated can be controlled by the micro-droplet size of the inner phase. In CEAs, the inner phase within the emulsion core and the emulsion core encapsulate by a soapy shell consisting of multi layer of surfactant molecules [23]. Therefore, when the stable

nucleus of cerium was formed it enlarged through the growth and aggregation of primary particles. As the particles reached the water droplets in inner phase the surfactant would cover the particles surface and hinder further particles growing, which also restricted the size of particles. Therefore, the emulsion droplet size prepared from the different methods was examined by dynamic light scattering (DLS) particle size distribution analysis, as shown in Figure 4.7. It was found that the emulsion droplet of CEAs was the smallest size.

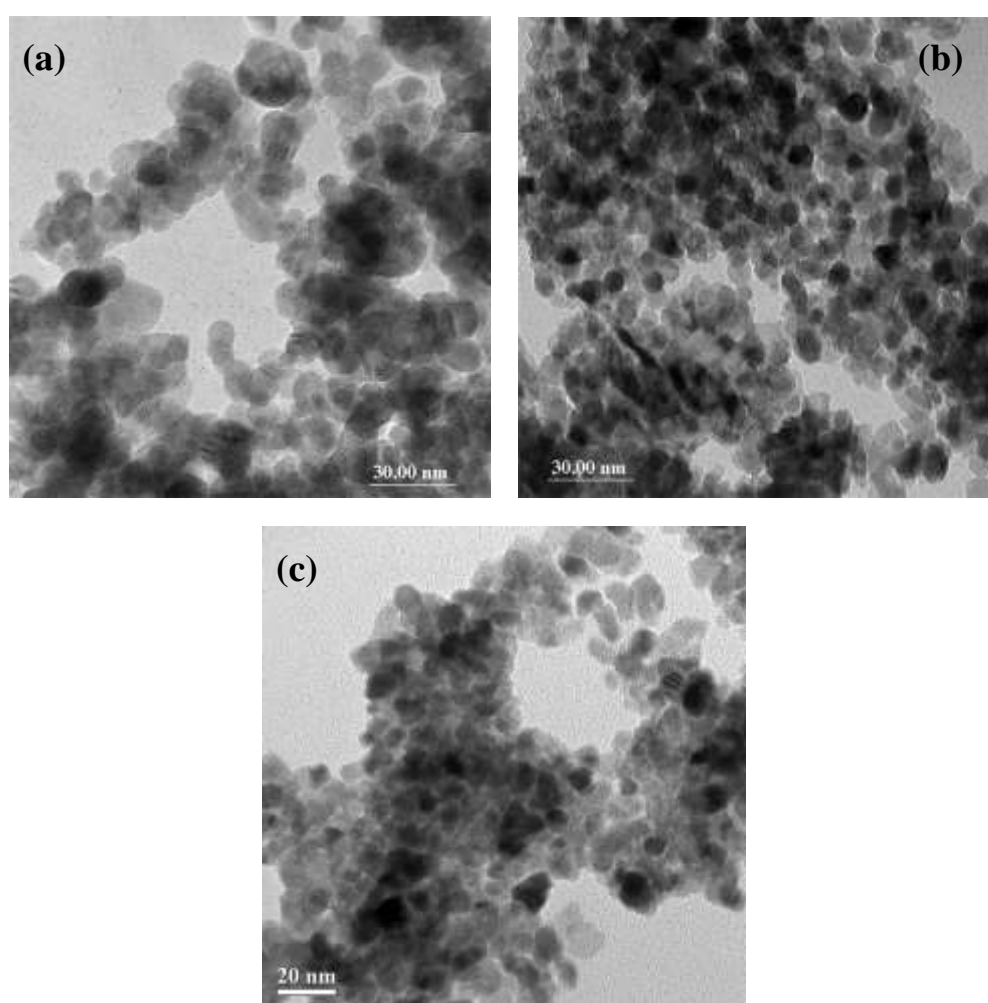


Figure 4.6 TEM micrograph of CeO_2 prepared by (a) RM, (b) ELM, and (c) CEAs.

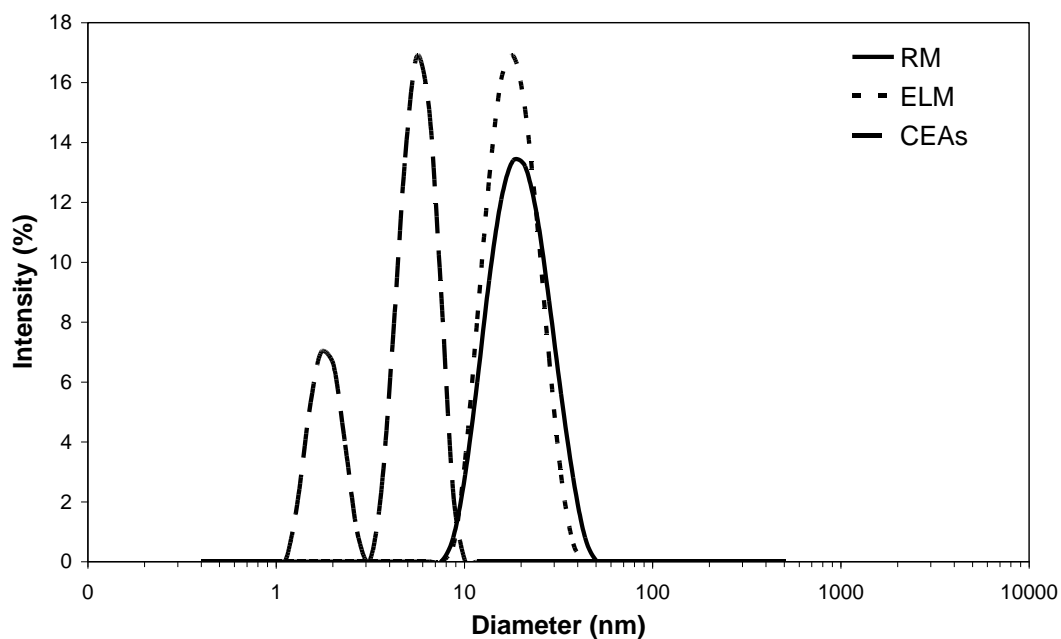


Figure 4.7 The emulsion droplet size distribution prepared by different methods.

The surface area of CeO_2 prepared by RM, ELM, and CEAs methods were 5.35, 9.77 and 145.7 m^2/g , respectively. The result showed that the surface area obtained from CEAs was higher than others method and shows higher percent yield. The porosity analysis were summarize in Table 4.1

The results from TEM, BET, and DLS indicated that CeO_2 prepared by CEAs method showed the smallest particle size, the highest surface area, and the smallest emulsion droplet which meant this method was suitable to prepared nano-sized particles.

Table 4.1 Surface area, porosity, average particle size, and percent yield of CeO_2 prepared by different methods.

Method	Surface area (m^2/g)	Pore volume (cm^3/g)	Pore size (\AA)	Average particle size (nm)	%Yield
RM	5.32	0.0548	411.8	9.4 ± 0.3	32.75
ELM	9.77	0.0673	275.5	5.8 ± 0.2	48.75
CEAs	145.73	0.2170	59.5	4.7 ± 0.1	84.29

The thermal analysis was carried out to evaluate the chemical composition of the CeO_2 and elucidate the transformation to crystalline CeO_2 . The thermo-gravimetric analysis of CeO_2 prepared by different emulsion method are given in Figure 4.8. TGA profile of CeO_2 obtained from RM and CEAs showed decomposition in two distinct states and three major weight losses were seen in TGA profile of CeO_2 obtained from ELM. TGA profile obtained from RM and CEAs showed initial weight loss at around 70-150°C and 80-150°C, respectively which associated with a mass loss of 5.36% and 2.73%, respectively and attributable to the loss of adsorbed water and crystal water. The second stage appear at 150-170°C and 150-300°C, respectively with a mass loss of 66.11% and 39.04%, respectively which represented decomposition of PE4LE to other organic compounds. CeO_2 obtained from ELM showed three major weight losses. The poorly resolved first step accounted for 1.94% weight loss up to 170°C due to the loss of adsorbed water. The second stage appears at 170-220°C with a mass loss of 16.51% and the last stage appears at 220-350°C with a mass loss of 6.29% it was attribute to the removal of PE4LE. The total weight loss of CeO_2 obtained from RM, ELM, and CEAs are 84.19, 26.06, and 44.97%, respectively.

All of TGA profile has no weight loss above 300°C indicating the crystalline CeO_2 formation as the final product. Therefore, CeO_2 obtained from three methods was calcined at 500°C are purity confirmed by TGA analysis.

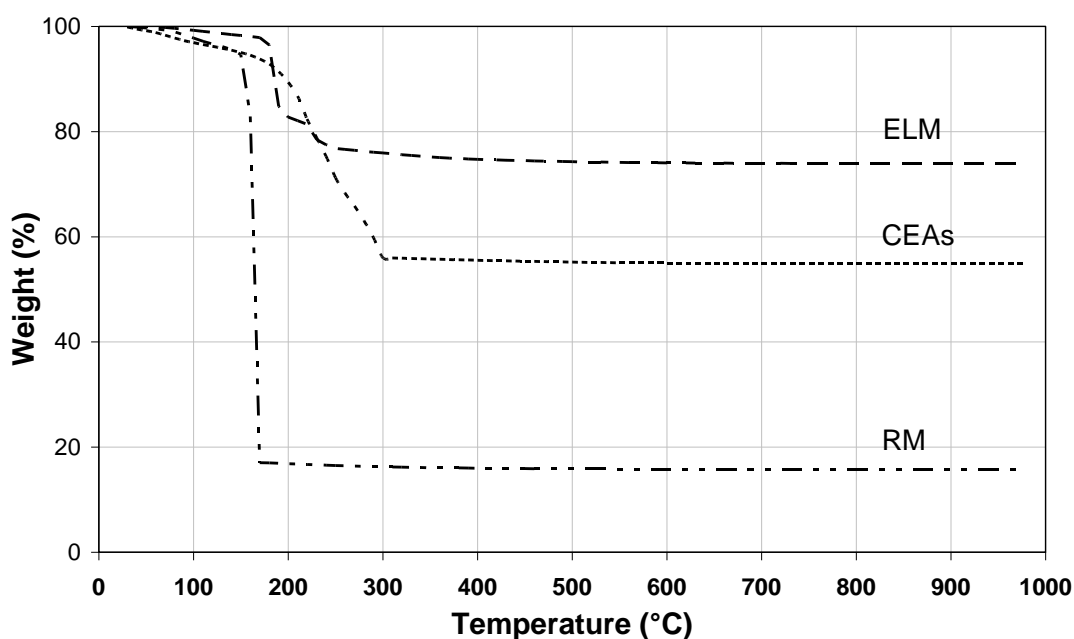


Figure 4.8 Thermo-gravimetric analysis of CeO_2 prepared by different methods.

4.5.2 Influence of various factors on the average particles size and surface area

4.5.2.1 The type of cerium source

Figure 4.9 shows the XRD patterns of the products prepared by CEAs method used different cerium sources. All the reflection in figure can be indexed to pure crystalline CeO_2 and no impurity peaks was observed in the patterns. The peaks was close to the ones of the face centered cubic fluorite structure of CeO_2 with lattice parameter is 5.4113 \AA (standard data JCPDS 34-0394).

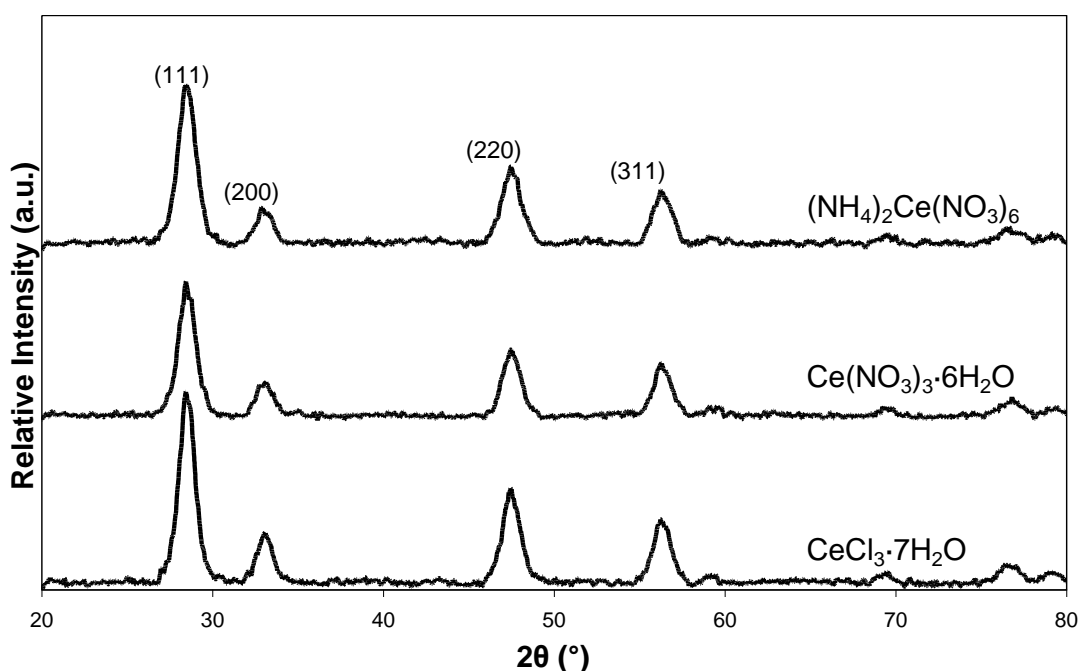


Figure 4.9 XRD patterns of CeO_2 prepared by CEAs using different cerium sources.

Figure 4.10 shows the TEM micrographs of CeO_2 prepared by CEAs method used different cerium source. It was evident from the figure that the particles were small in size and uniform in shape. The average particle size of CeO_2 obtained from $(\text{NH}_4)_2\text{Ce}(\text{NO}_3)_6$, $\text{Ce}(\text{NO}_3)_3 \cdot 6\text{H}_2\text{O}$ and $\text{CeCl}_3 \cdot 7\text{H}_2\text{O}$ as a cerium source were 4.7, 5.4 and 5.9, respectively. However, this result shows that the average particles size of CeO_2 obtained from $(\text{NH}_4)_2\text{Ce}(\text{NO}_3)_6$ (in Figure 4.10 (a)) was the smallest.

Consider the average size of CeO_2 particles with different cerium sources it was found that the average size obtained from $(\text{NH}_4)_2\text{Ce}(\text{NO}_3)_6$ was the smallest and the average

size obtained from $\text{Ce}(\text{NO}_3)_3 \cdot 6\text{H}_2\text{O}$ was smaller than that from $\text{CeCl}_3 \cdot 7\text{H}_2\text{O}$. It could be explained that $(\text{NH}_4)_2\text{Ce}(\text{NO}_3)_6$ has lower surface tension than the others. An experiment was carried out by dropping the same concentration solution of $(\text{NH}_4)_2\text{Ce}(\text{NO}_3)_6$, $\text{Ce}(\text{NO}_3)_3 \cdot 6\text{H}_2\text{O}$ and $\text{CeCl}_3 \cdot 7\text{H}_2\text{O}$ on glass surface, it was found that a droplet of $\text{CeCl}_3 \cdot 7\text{H}_2\text{O}$ showed less flat shape than the others which meant $\text{CeCl}_3 \cdot 7\text{H}_2\text{O}$ has the higher surface tension. Cerium compound that has low surface tension, can disperse to small droplets in emulsion easily, as a result, the small particles are produced.

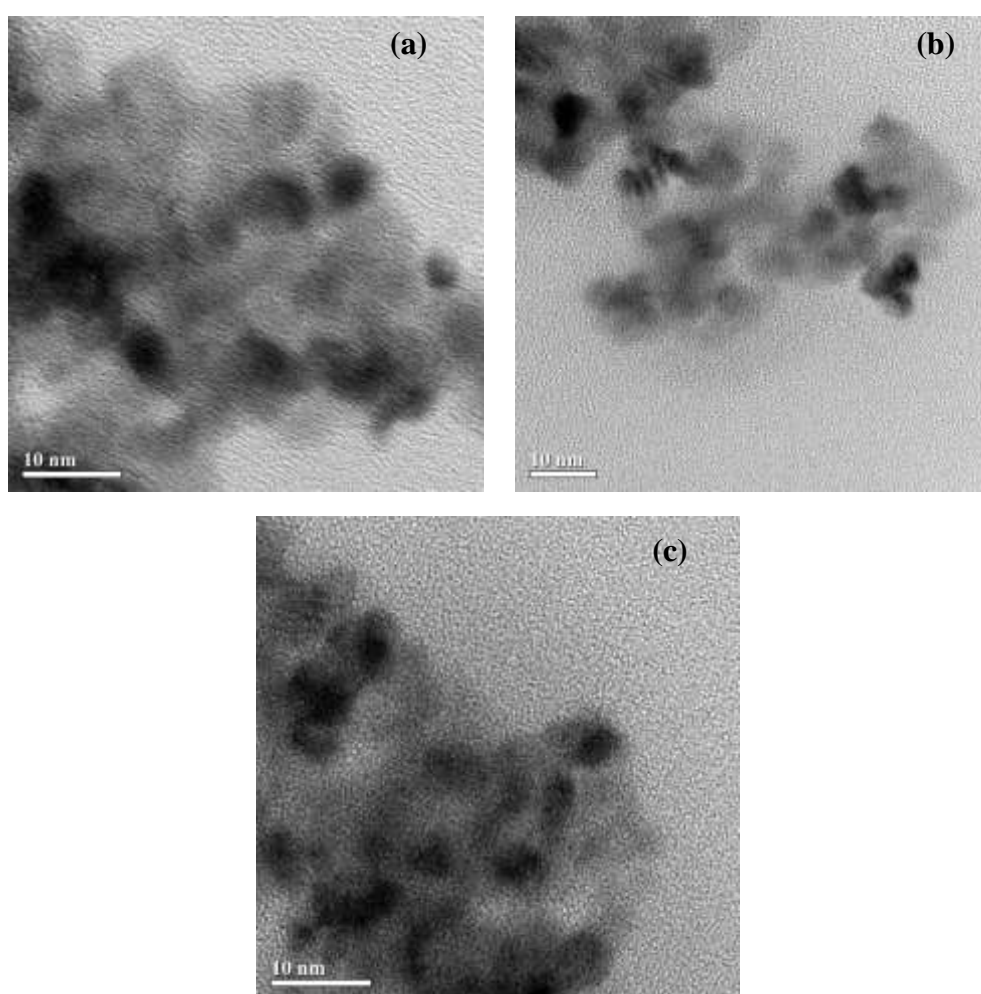


Figure 4.10 TEM micrographs of CeO_2 prepared by CEAs method using different cerium sources (a) $(\text{NH}_4)_2\text{Ce}(\text{NO}_3)_6$, (b) $\text{Ce}(\text{NO}_3)_3 \cdot 6\text{H}_2\text{O}$, and (c) $\text{CeCl}_3 \cdot 7\text{H}_2\text{O}$.

The surface area of CeO_2 prepared by CEAs method used $(\text{NH}_4)_2\text{Ce}(\text{NO}_3)_6$, $\text{Ce}(\text{NO}_3)_3 \cdot 6\text{H}_2\text{O}$ and $\text{CeCl}_3 \cdot 7\text{H}_2\text{O}$ as cerium source were 145.7, 138.8 and 139.5 m^2/g ,

respectively. The result shows that the surface area nearly the same. On the other hand, surface area obtained from $(\text{NH}_4)_2\text{Ce}(\text{NO}_3)_6$ was higher than the others and shows higher percent yield. The porosity analysis were summarize in Table 4.2.

Table 4.2 Surface area, porosity, average particle size and percent yield of CeO_2 prepared by different cerium sources.

Cerium source	Surface area (m^2/g)	Pore volume (cm^3/g)	Pore size (\AA)	Average particle size (nm)	%Yield
$(\text{NH}_4)_3\text{Ce}(\text{NO}_3)_6$	145.7	0.217	59.5	4.7 ± 0.1	84.29
$\text{Ce}(\text{NO}_3)_3 \cdot 6\text{H}_2\text{O}$	138.8	0.244	69.8	5.4 ± 0.2	81.21
$\text{CeCl}_3 \cdot 7\text{H}_2\text{O}$	139.5	0.204	58.3	5.9 ± 0.5	69.97

4.5.2.2 The type of surfactant

Figure 4.11 shows the XRD patterns of the products prepared by CEAs method used different surfactants. All the reflection in Figure 4.11 could be indexed to pure crystalline CeO_2 and no impurity peaks was observed in the patterns. The peaks was close to the ones of the face centered cubic fluorite structure of CeO_2 with lattice parameter is 5.4113 \AA (standard data JCPDS 34-0394).

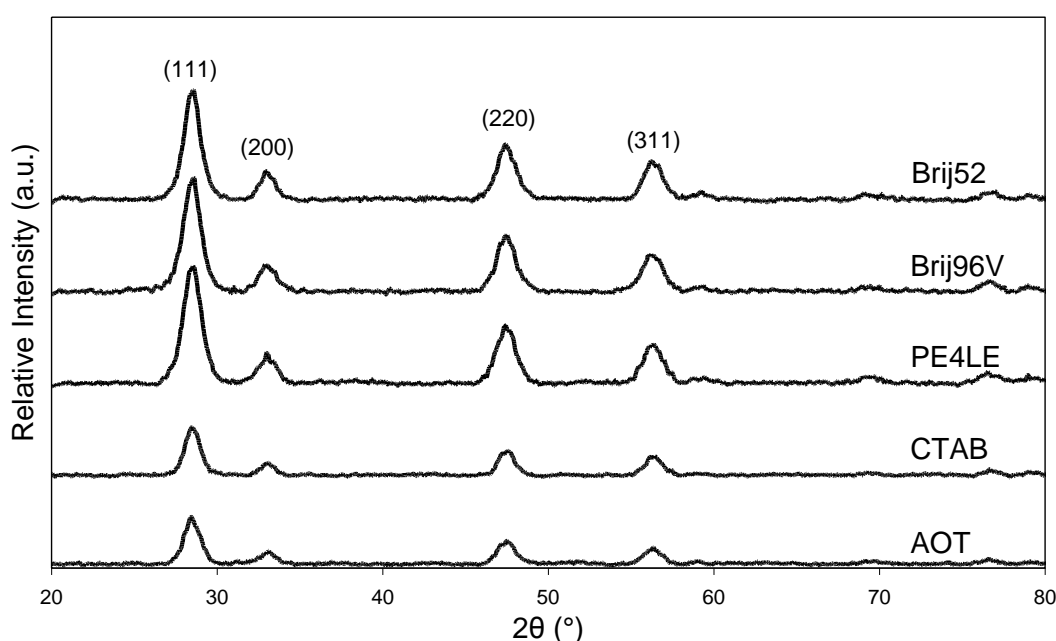


Figure 4.11 XRD patterns of CeO_2 prepared by CEAs using different surfactants.

Figure 4.12 shows the TEM micrographs of CeO₂ prepared by CEAs method used different surfactant. It is evident from the figure that the particles were small in size and uniform in shape. The average particle size of CeO₂ obtained from PE4LE, Brij96V, Brij52, AOT and CTAB were 4.7, 4.5, 4.6, 4.1 and 5.1, respectively. However, this result shows that the average particles size of CeO₂ obtained from AOT (in Figure 4.12 (d)) was the smallest.

The effect of the hydrophobic group of surfactant on the CeO₂ particle size was investigated in the CEAs method using nonionic surfactants. When considering the average size of CeO₂ particles with different nonionic surfactants it was found that the average size obtained from Brij96V was the smallest. The average size obtained from Brij52 was smaller than that from PE4LE. The studied surfactants are nonionic surfactant but Brij96V has the longest hydrocarbon chain (HC) length. If the hydrophobic hydrocarbon chain length is longer, the solubility of the surfactant in water decreases and its solubility in n-hexane increases [51], and surfactant tend to form aggregates which is call micelles. Since there are more micelles formed and the amount of water is the same, the size of water droplets in micelles are smaller resulting in smaller sizes of the particles. However, Brij96V shows the smallest average particle size but it difficult to form emulsion and used amount more than PE4LE to form emulsion at the same condition.

The average particle size of CeO₂ prepared by using PE4LE and CTAB were 4.7 and 5.1 nm, respectively, while the particles prepared by using AOT were as small as 4.1 nm. It was considered that as the cerium ion has positive charge, AOT showed strongly adsorbed on the surface but CTAB might not adsorbed on surface. A certain repellent action exists between the hydrophilic group of CTAB and cerium cation at grain surface, which makes the stabilizing effect of CTAB on grain become weaker [33]. When nonionic surfactant (PE4LE) was used, the average particle size of CeO₂ were bigger than anionic surfactant. This result showed be attribute to stabilizing effect of nonionic surfactant on water droplets and particles mainly derives from its hydrogen bond with water [6]. This action is weaker than that of ion bond.

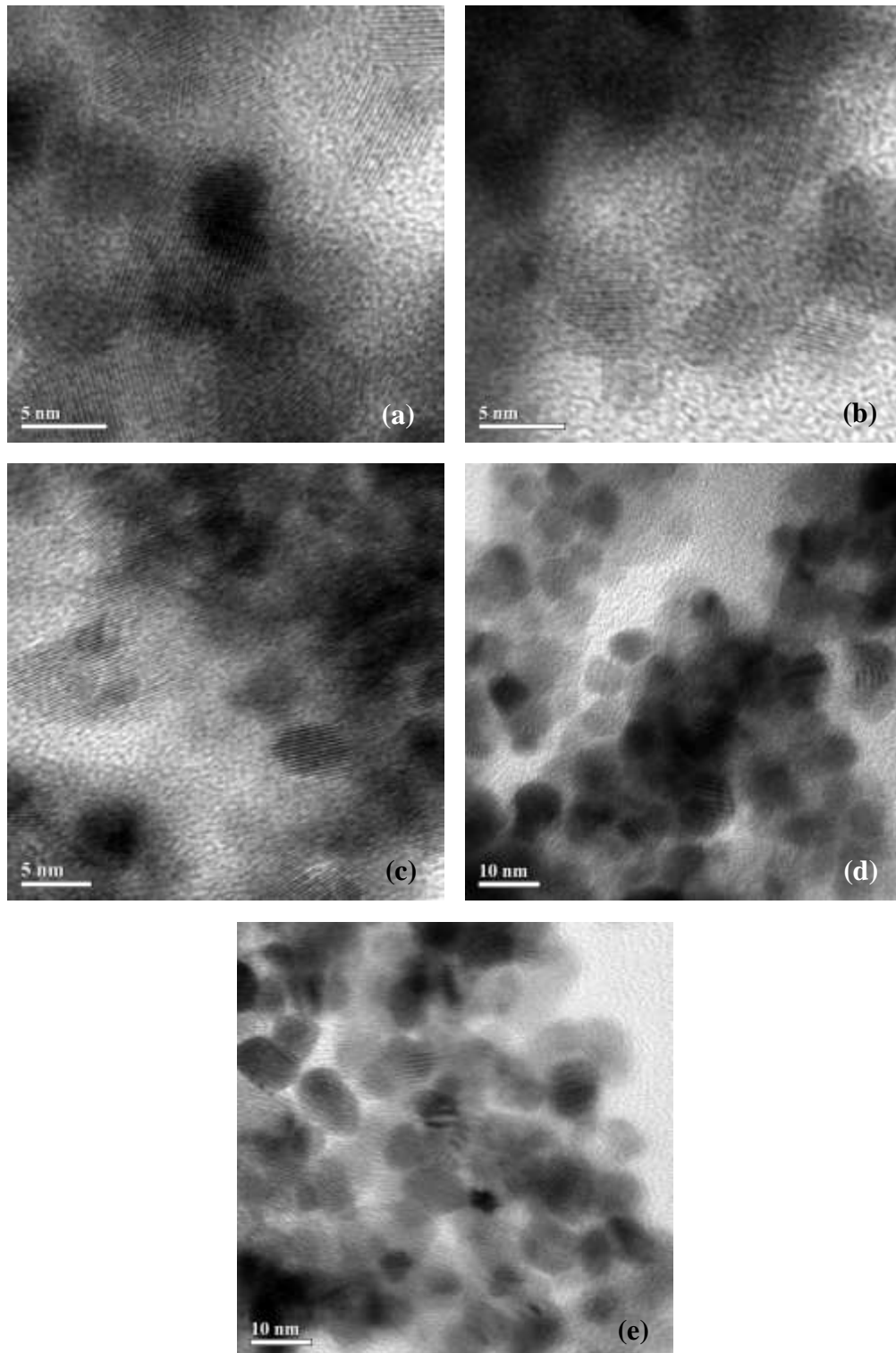


Figure 4.12 TEM micrographs of CeO₂ prepared by CEAs method using different surfactants (a) PE4LE, (b) Brij96V, (c) Brij52, (d) AOT, and (e) CTAB.

The surface area of CeO₂ prepared by PE4LE, Brij96V, Brij52, AOT, and CTAB were presented in Table 4.3. The result shows that the surface area obtained from Brij96V were the highest.

Table 4.3 Surface area, porosity, average particle size and percent yield of CeO₂ prepared by different surfactants.

Surfactant	Surface area (m ² /g)	Pore volume (cm ³ /g)	Pore size (Å)	Average particle size (nm)	% Yield
PE4LE	145.7	0.217	59.55	4.7 ± 0.1	84.29
Brij96V	154.8	0.345	89.15	4.5 ± 0.2	78.30
Brij52	148.4	0.215	57.99	4.6 ± 0.1	78.38
AOT	102.5	0.171	66.65	4.1 ± 0.2	84.06
CTAB	34.6	0.115	132.70	5.1 ± 0.1	95.33

4.5.3.3 The calcinations temperature

Figure 4.13 shows the XRD patterns of the products prepared by CEAs method carried out at different calcinations temperature. All the reflection in Figure 4.13 could be indexed to pure crystalline CeO₂ and no impurity peaks was observed in the patterns. The peaks was close to the ones of the face centered cubic fluorite structure of CeO₂ with lattice parameter is 5.4113 Å (standard data JCPDS 34-0394).

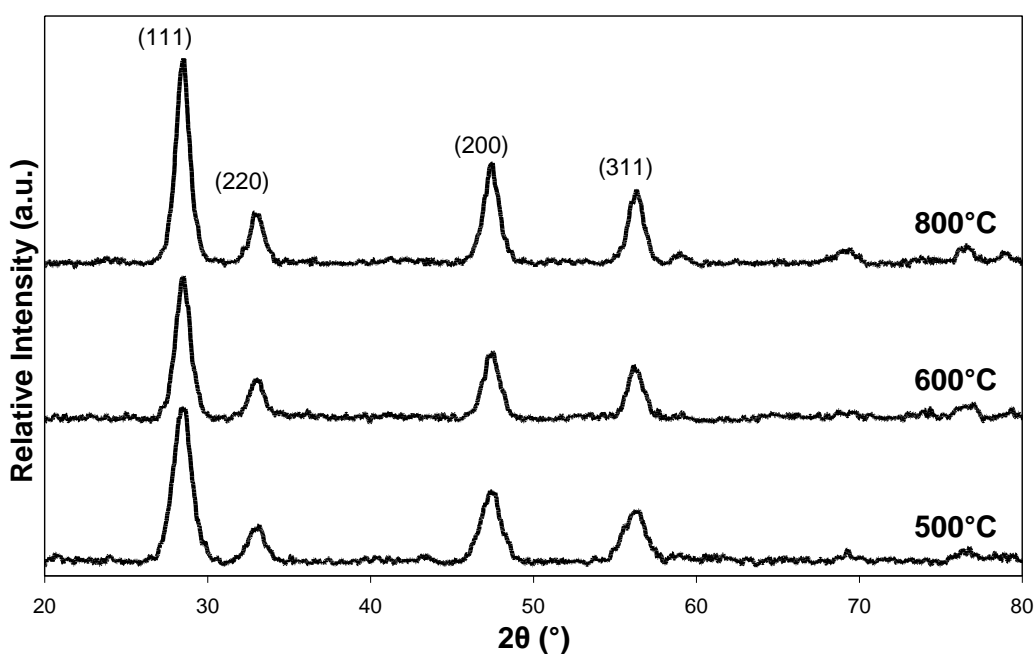


Figure 4.13 XRD patterns of CeO₂ prepared by CEAs method at different calcinations temperature.

Table 4.4 Total pore volume, surface area and average pore diameter of CeO₂ prepared by CEAs method at different calcinations temperature.

Catalyst	Pore volume (cm ³ /g)			Surface area (m ² /g)			D (Å)
	V _T	V _{me}	V _{mi}	S _{BET}	S _{me}	S _{mi}	
CeO ₂ (100°C)	0.1273	0.0278	0.0995	201.4	25.9	175.5	25.3
CeO ₂ (200°C)	0.1781	0.1427	0.0354	175.3	164.0	11.3	38.7
CeO ₂ (300°C)	0.1248	0.1006	0.0242	159.6	154.5	5.1	31.3
CeO ₂ (400°C)	0.2155	0.2126	0.0029	155.7	147.8	7.9	55.4
CeO ₂ (500°C)	0.2170	0.2158	0.0012	145.7	145.4	0.3	58.5
CeO ₂ (600°C)	0.1747	0.1687	0.0060	137.7	137.5	0.2	69.8
CeO ₂ (900°C)	0.0470	0.0470	0.0000	47.6	47.6	0.0	114.9

V_T: Total pore volume, *V_{me}*: Mesopore volume, *V_{mi}*: Micropore volume,

S_{BET}: BET surface area, *S_{me}*: Mesopore surface area, *S_{mi}*: Micropore surface area,

D: Average pore diameter.

Table 4.4 summarizes the results of specific surface area, pore volume and average pore diameter of CeO₂ at different calcinations temperature. It was observed that after drying, specific surface area (*S_{BET}*) of CeO₂ was 201.40 m²/g and surface area decreased at high calcination temperature. The results of total pore volume (*V_T*) showed similar trend as of *S_{BET}*. The decrease of micropore surface area (*S_{mi}*) with increasing of calcination temperature was also observed. It may be ascribed to the sintering impact.

Figure 4.14 shows the TEM micrographs of CeO₂ prepared by CEAs method carried out at different calcinations temperature in the range of 500-800°C. The average particle size of CeO₂ obtained from the calcination temperature of 500, 600, and 800°C were 4.7, 7.6, and 14.9 nm, respectively. The average particle size of CeO₂ increased sharply with the rise of calcinations temperature. The observation could be explained as with the increase of calcination temperature, the growth rate of particles increases more rapidly than the nucleation rate does, and the aggregation trend of particles becomes stronger [6].

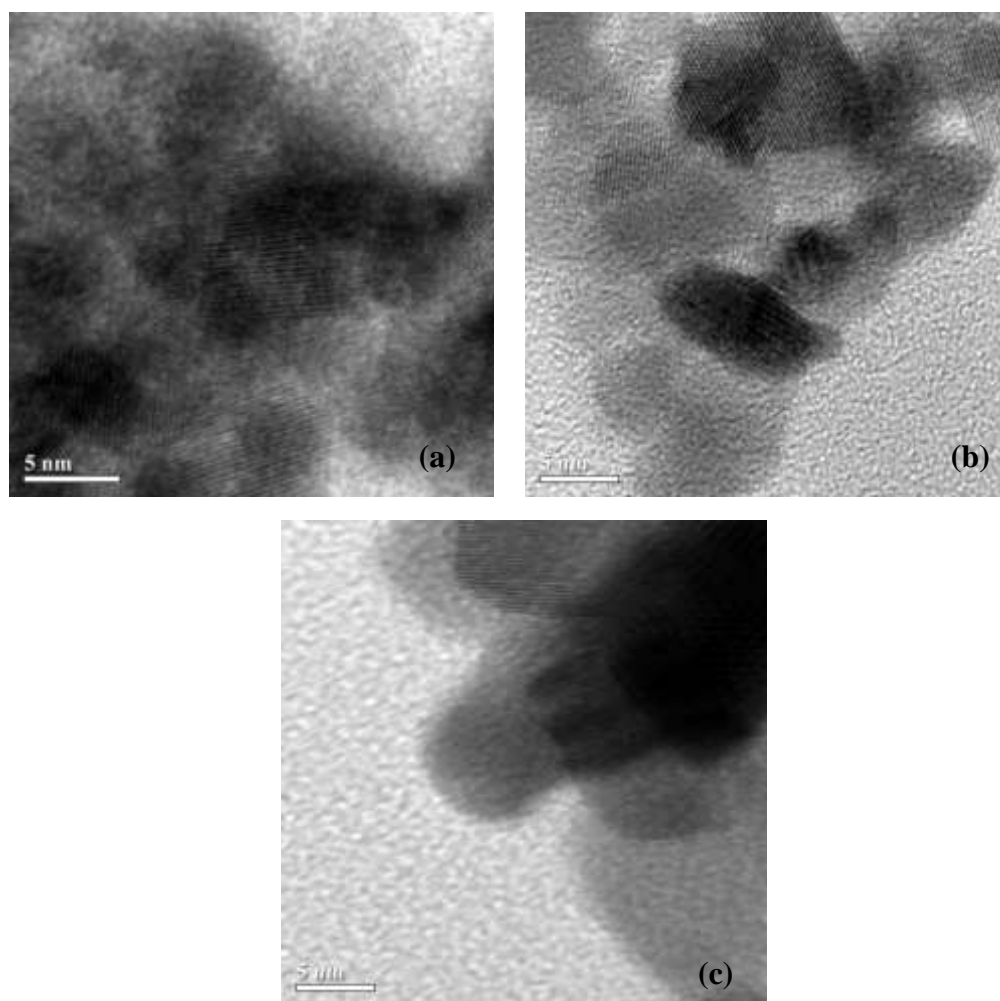


Figure 4.14 TEM micrograph of CeO₂ prepared by CEAs method at different calcinations temperature (a) 500°C, (b) 600°C and (c) 800°C.

4.5.3.4 The water content

Figure 4.15 shows the XRD patterns of the products prepared by CEAs method carried out at different calcinations temperature. All the reflection in Figure 4.15 could be indexed to pure crystalline CeO₂ and no impurity peaks was observed in the patterns. The peaks were close to the ones of the face centered cubic fluorite structure of CeO₂ with lattice parameter is 5.4113 Å (standard data JCPDS 34-0394).

The effects of water content are shown in Table 4.5. From table it was found that the crystallite size of CeO₂ was affected by water content. At water content of 3, 5 and 7 ml, the crystallite size were 5.81, 5.91 and 6.45 nm, respectively (calculated by equation (4.2)). The increase of water at constant concentration of surfactant caused the increase

of crystallite size. This observation could be explained that the size of the final particle much depend on the size of the droplets in the emulsion core which were influenced by the water content [52]. At high water content, there are more free water molecules in CEAs resulting in the interfacial rigidity is poorer as compared with at lower water content. These lead to enhance the exchange rate of reactants among micelles and widen the particle size distribution. So, it could be rationalized that the presence of free water in the CEAs provides morphological tailoring of particles [51].

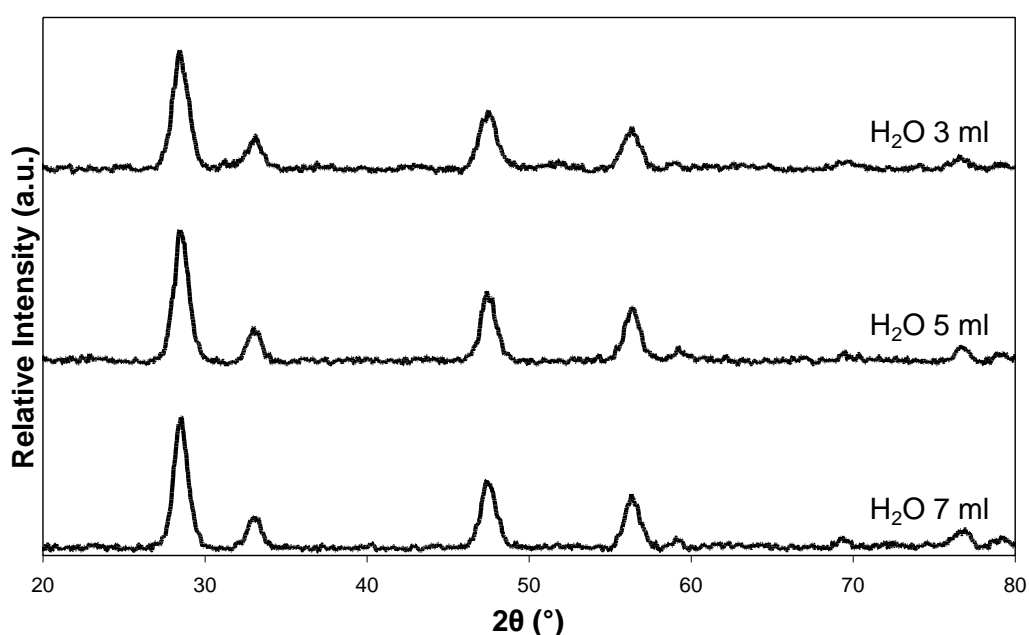


Figure 4.15 XRD patterns of CeO₂ prepared by CEAs method at different water content.

Table 4.5 Surface area, porosity, average particle size and percent yield of CeO₂ prepared by CEAs method at different water content.

Water content (ml)	Surface area (m ² /g)	Pore volume (cm ³ /g)	Pore size (Å)	Crystallite size (nm)	% Yield
3	145.73	0.2170	59.5	5.81	84.29
5	102.9	0.2174	84.5	5.91	84.47
7	94.5	0.1804	76.4	6.45	87.78

4.6 Summary

Nano-sized CeO₂ was successfully prepared by different emulsion methods. The results from XRD, TEM and BET measurement indicated that the obtained particles were cubic fluorite structure CeO₂ nanoparticles. The preparation by colloidal emulsion aphrons method using (NH₄)₃Ce(NO₃)₆ as a cerium source, PE4LE as a surfactant and three milliliter of water content was chosen as the suitable condition for produced CeO₂ nanoparticles with the highest surface area and the smallest particle size. The surface tensions of cerium solution have effect on the particle size. The hydrocarbon chain lengths of nonionic surfactant have affection of solubility in emulsion and could be decrease in particle size. A mutual repulsion between hydrophilic group of the cationic surfactant and nanoparticle surface might be weaker, as a result, CeO₂ particles became larger than that used nonionic surfactant. Calcinations in higher temperature make the average size of products increasing. By increasing the water content the final particle of CeO₂ was increased.